Creep and creep recovery of cast aluminum alloys

Jay Christian Dandrea · Roderic Lakes

Abstract Constant load uniaxial creep tests were performed on four aluminum alloys (designated M4032-2, 332, 332RR, and 333) at stresses of 31.5 MPa, 56.5 MPa, and 73 MPa and temperatures of 220°C and 260°C. Of the four materials, M4032-2 had the greatest resistance to creep, while 332RR alloy had the least. In addition to creep, the creep recovery phase was observed as well. It was found that, even for short loading periods, much of the time-dependent strain was not recoverable for all of the materials studied. Hardening was observed to occur in each of the alloys, resulting in a reduced creep rate on subsequent loadings. A constitutive equation for creep and recovery incorporating both stress and temperature dependence was developed for each of the alloys tested based on a viscous-viscoelastic model.

Keywords Creep · Recovery · Aluminum alloy · Cast · Small engine

1 Introduction

A number of components in small engines are constructed from cast aluminum alloys, despite the tendency of such materials to exhibit relatively poor creep performance. Common production processes currently used include high pressure die-casting, permanent mold casting, and lost foam casting. Alloy composition typically varies with manufacturer, and different alloys may be used by the same manufacturer for different components. Creep of these materials becomes a significant problem in air cooled engines due to their high operating temperatures, and can lead to component failure, loss of tolerances, and bolt load loss in bolted joints. The result of this is an engine with decreased efficiency, increased emissions, oil leaks, and increased maintenance requirements.

J.C. Dandrea · R. Lakes (✉)
Department of Engineering Physics, University of Wisconsin-Madison, Madison, WI 53706, USA
e-mail: lakes@engr.wisc.edu

J.C. Dandrea
e-mail: jaycdandrea@gmail.com

In the interest of meeting increasingly strict emissions standards and the public demand for maintenance free equipment, it becomes necessary for the manufacturer to seek out materials that exhibit increased creep performance (i.e. less creep). Due to the cost sensitive nature of small engines, the use of exotic materials is forbidden. New materials must be selected from those that are readily available and components must be able to be easily manufactured on a large scale. Changes in composition and processing can have a significant influence on the high temperature properties, but creep data for such materials is sparse. The performance of the materials can be evaluated from simple constant load uniaxial creep test data, from which engineers can then use to select the best material and process combinations possible. Constitutive equations created from the uniaxial test data can be used by engine designers to predict bolt load loss in bolted joints (Jaglinski et al. 2007).

In the current work, the time-dependent behavior of three permanent mold cast aluminum alloys and one die-cast aluminum alloy provided by two different engine manufacturers is evaluated through a set of uniaxial constant load creep tests. The creep recovery of the materials is observed as well, as it is considered that the recovery of the material plays a role in the load loss in a bolted joint. Constitutive equations, incorporating both stress and temperature dependence are developed for each material.

2 Experimental methods and materials

Test specimens of four alloys (designated M4032-2, 332, 332RR, and 333) were received from the manufacturers. The 332, 332RR, and 333 alloys all originated from the same source and were produced from a permanent mold process, while the high pressure die-cast M4032-2 alloy was received from a second manufacturer. The compositions of the materials are given in Table 1. A post-processing heat treatment step was specified for 332, 332RR, and 333 alloys in which the 332 and 333 alloys were placed in a preheated 288°C (550°F) oven for 3 hours, while 332RR alloy was subjected to 316°C (600°F) for 2 hours.

Additional machining and threading of the 332, 332RR, and 333 specimens was required in order to allow them to fit into the test frame using available fixtures. Previous work had shown that removal of the die-cast skin layer had no effect on creep rate (Nimityongskul 2005). The final gage length of these materials was 4.5″ with a diameter of 0.3″. Specimens of M4032-2 alloy had a gage length of 3.4″, a diameter of 0.25″, and could be tested as-received.

Constant load uniaxial creep tests were conducted using a dead weight lever frame (Riehle M20101-R). The specimen was heated with a tube furnace attached to the creep frame. Constant temperature was maintained through use of a temperature controller, which received input from a thermocouple attached to the test specimen with high temperature tape.

Table 1 Composition of 332, 333, 332RR, and M4032-2 alloys

	Si	Fe	Cu	Mn	Mg	Ni	Zn	Ti	Pb	Sn	Cr
332	8.91	0.66	3.13	0.32	1.13	0.10	0.45	0.17	0.02	0.01	0.04
333	8.79	0.64	3.08	0.31	0.21	0.10	0.45	0.13	0.02	0.01	0.04
332RR	9.69	0.77	3.41	0.13	1.08	1.13	0.10	0.10	0.01	0.01	0.03
M4032-2	14		4			2					

Strain was measured using a full bridge circuit of strain gages (WK 350 Ω, Vishay Micro-Measurements). Two gages were fixed to opposite sides of the stressed specimen to eliminate effects of possible bending, and two gages were attached to an unstressed "dummy" specimen to account for thermal expansion. The bridge was interfaced with an Apple Macintosh IIci computer to allow for automated data collection. Application of the load was performed by lowering of a jack, while removal of the load was accomplished by manually lifting the load and placing it back onto the raised jack. Both application and removal of the load took less than 10 seconds. Data collection began after the initial ramp up period and was collected using a LabView (version 2.2.1) virtual instrument capable of recording data on a logarithmic time scale with a time resolution of 1 second.

Creep tests were performed at an initial stress of 31.5 MPa, 56.5 MPa, and 73 MPa, with one test at each stress completed at both 220°C and 260°C. The stresses correspond to approximately 25%, 50%, and 75% of the yield stress of a typical die-cast aluminum alloy, while the temperatures are believed to be representative of engine operating temperatures. For each combination of stress and temperature, the specimen was loaded, in succession, for periods of 100 seconds, 1000 seconds, 10000 seconds, and 100000 seconds. Following each period of creep, the load was removed and the creep recovery of the specimen observed for one decade of time beyond the length of time that the specimen had been loaded. The same specimen was used for each set of tests at a given stress and temperature. The loading times were chosen to represent a typical high temperature loading cycle in the applications that the materials are intended for. A lawn mower engine may be typically operated for 1000–10000 seconds at a time, a motorcycle for a few hours, and a generator may run continuously for a day.

Due to the weight of the frame fixtures attached to the lower end of the test specimen, the recovery phase of the tests does not occur under zero load. The weight of this assembly is 16.9 lbs, which corresponds to a stress of 2.4 MPa for a $1/4''$ diameter specimen. It was assumed that this stress is small enough that no measurable creep occurs due to this load over the times observed, and that the strain resulting from it is elastic in nature and can be subtracted from the results. This was confirmed by installing a new specimen in the test frame and recording the change in strain at 220°C with the only load being that of the lower control arm assembly. After one day, the total change in strain was $4.8\mu\varepsilon$ in the compressive direction. Since the load places the material in tension, it is verified that no measurable creep is occurring over this time frame under this load and that the change in strain should be attributed to drift.

3 Results and discussion

The creep and creep recovery results for 332 alloy for the entire range of tests is presented in Fig. 1. Minimal recovery was observed for time beyond the length of time that the specimen had been loaded, so in order to allow for both creep and recovery to be observed on the same plot, recovery results are only shown for the same length of time as the creep test. Due to the large number of tests involved, the entire range of data is only shown for 332 alloy (Fig. 1). The full data for each of the materials is given in Dandrea (2008).

For the creep tests at 56.5 MPa and 73 MPa, the initial strain is much larger in Fig. 1a than it is in Figs. 1b–1d, suggesting that the yield strength of this alloy is greatly reduced at high temperature. This plastic strain occurred in 332RR and 333 alloys as well, but not in M4032-2 alloy. Also, even at the lowest stress and for short loading times, it is observed that much of the time-dependent strain accrued during loading is not recoverable. This characteristic was observed in all four alloys.
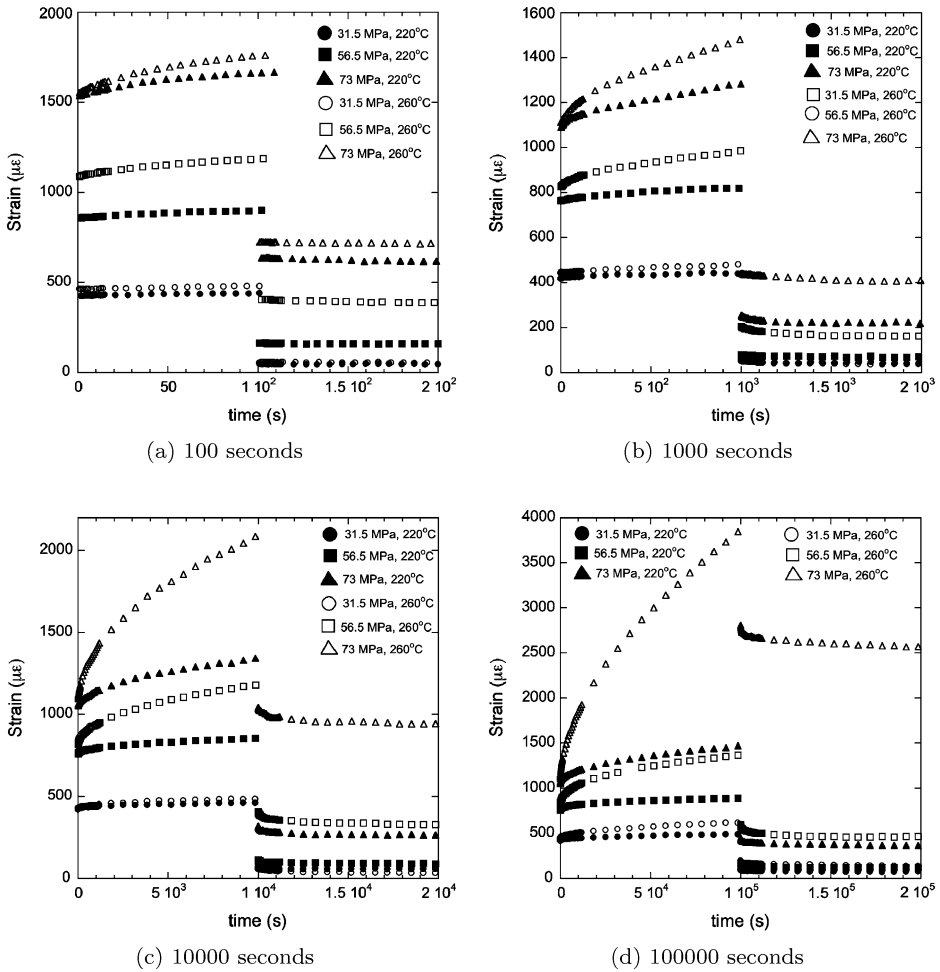
Fig. 1 Creep and recovery of 332 alloy at 220°C and 260°C for loading times of 100 s, 1000 s, 10000 s, 100000 s

Repeated loading of the same specimen revealed that hardening, indicated by a decreasing creep rate on subsequent loadings, occurred in all of the materials tested. This is shown for 332 alloy at 260°C in Fig. 2. The effect was much more pronounced for 332, 332RR, and 333 alloys than it was for M4032-2 alloy. This hardening is beneficial in that components in an engine that has been subjected to some use will exhibit less creep than those in a new one, suggesting that the introduction an initial conditioning step or re-tightening a joint at some initial prescribed interval, will improve the long term performance of the engine.

3.1 Modeling

In previous works (Jaglinski and Lakes 2004; Jaglinski et al. 2007), the creep behavior of die-cast aluminum alloys has been modeled using the a form of the Andrade equation for

Fig. 2 Creep of 332 alloy at 260°C. strain rate is decreasing on successive loadings
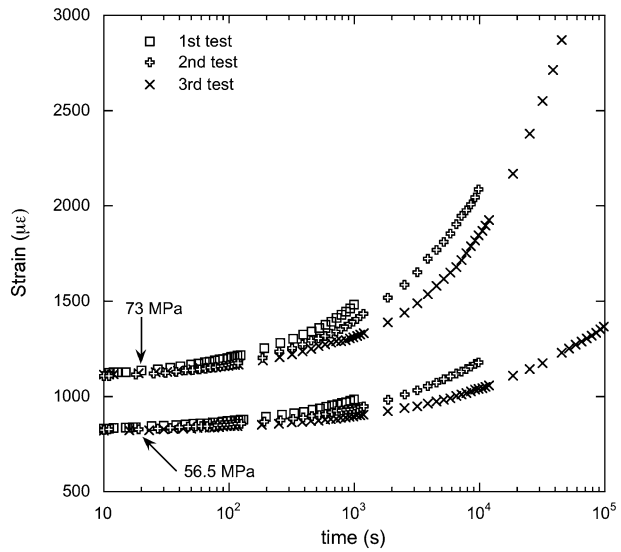
creep (Andrade 1910)

$$\varepsilon(t) = \varepsilon_\circ + A(\sigma)t^n \qquad (1)$$

where for primary creep $n < 1$. The time scale in Fig. 2 is logarithmic; the creep is primary. Application of the modified superposition principle (Findley and Lai 1967) to the above equation predicts that if the load is removed at time t_1, the recovery phase will be given by

$$\varepsilon(t) = A(\sigma)[t^n - (t - t_1)^n] \quad t > t_1 \qquad (2)$$

Similar models are widely used to industry to calculate creep, however it is apparent that, while (1) may be able to accurately represent the creep of such materials, the above method incorrectly predicts the creep recovery phase of the materials tested here since (2) predicts that the creep strain is anelastic and will fully recover after the load has been removed. The back stress approach was not used because in the stress regime used here, there is a continuous transition between linear viscoelasticity with minimal creep at small stress to nonlinearity at higher stress. The back stress approach gives an abrupt effect which neglects the small stress regime. A viscous-viscoelastic model (Findley and Lai 1978; Cho and Findley 1980, 1982, 1984; Ding and Findley 1985) suggests that the time-dependent strain can be separated into a recoverable viscoelastic component ε_{ve} and a nonrecoverable "viscous" component ε_v. The total strain during loading is then given by

$$\varepsilon(t) = \varepsilon_\circ + \varepsilon_{ve} + \varepsilon_v \qquad (3)$$

where $\varepsilon_\circ$ is a combination of time-independent elastic and plastic strains that occur instantaneously upon loading, and in the absence of yielding, for a uniaxial applied stress, $\varepsilon_\circ = \sigma/E$ where E is Young's Modulus. Since the creep strain during loading can be represented by $A(\sigma)t^n$, as given in (1), both ε_{ve} and ε_v were taken to have the same form. The total strain during loading is then

$$\varepsilon(t) = \varepsilon_\circ + B(\sigma)t^N + C(\sigma)t^n \qquad (4)$$

It is assumed that superposition applies to the viscoelastic strain, while by definition, ε_v is permanent. The creep recovery following removal of the load at time t_1 will then follow

$$\varepsilon(t) = B(\sigma)t_1^N + C(\sigma)[t^n - (t - t_1)^n] \quad t > t_1 \tag{5}$$

It was found that the creep behavior of each of the materials could be well represented by (1) with $n = 1/3$. For simplicity, it was then taken that $N = n = 1/3$. The permanent strain $B(\sigma)t_1^N$ was determined by fitting the recovery data to (5). The viscoelastic component was then determined by fitting equation (4) to the creep data. Young's Modulus was determined by plotting the elastic strain $\varepsilon_\circ$ measured on unloading from the 220°C tests versus stress and performing a linear fit to the data. It is noted that since the load cannot be applied or removed instantaneously and strain cannot be accurately measured at very short times using the methods here, the E determined here is more of a fitting parameter. The values of E obtained for M4032-2, 332, 332RR, and 333 alloys were found to be 77.5 GPa, 72.8 GPa, 71.2 GPa, and 73.9 GPa, respectively.

Previous creep models for die-cast aluminum alloys had been temperature specific (Jaglinski and Lakes 2004; Jaglinski et al. 2007). The effects of temperature can be incorporated by replacing the time variable t with the temperature compensated time θ introduced by Sherby et al. (1954)

$$t \to \theta = \int_0^t e^{-Q/RT(s)} ds \tag{6}$$

where Q is the activation energy for creep, R is the gas constant, and T is the absolute temperature. For creep at a constant temperature, (1) becomes

$$\varepsilon(t) = \varepsilon_\circ + A(\sigma)e^{-nQ/RT}t^n \tag{7}$$

The strain rate is then given by $\dot{\varepsilon} = nA(\sigma)e^{-nQ/RT}t^{n-1}$. By performing two tests at the same stress level at two different temperatures T_1 and T_2, the activation energy can then be determined by taking the ratio $\dot{\varepsilon}(T_1)/\dot{\varepsilon}(T_2)$

$$\ln\left[\frac{\dot{\varepsilon}(T_1)}{\dot{\varepsilon}(T_2)}\right] = \frac{nQ}{R}\left(\frac{1}{T_2} - \frac{1}{T_1}\right) \tag{8}$$

The creep activation energy Q was calculated by fitting the experimental creep data to (7) with $n = 1/3$. The apparent activation energies at each stress for the four materials tested are shown in Table 2. For 332RR alloy, the creep activation energy is roughly constant over the entire stress range. For the M4032-2 and 333 alloys, Q is approximately constant at 31.5 MPa and 56.5 MPa and increases by a large amount at 73 MPa. The apparent activation energies are similar at 56.5 MPa and 73 MPa for 332 alloy, and much lower at 31.5 MPa. The jump in activation energy suggests that at high stress additional processes begin to contribute to creep in the materials.

In construction of the viscous-viscoelastic model for the four alloys, the activation energy was taken as the average of the values of the activation energies in Table 2 over the stress range in which Q is approximately constant. This has the negative effect of reducing the accuracy of the model at high stress, however due to the large amount of creep exhibited by all of the materials tested at the highest stress (Dandrea 2008), it is unlikely that they should be subjected to such conditions in the applications for which they are intended.

The stress functions $B(\sigma)$ and $C(\sigma)$ were chosen to be represented by power series of the form $B(\sigma) = B_1\sigma + B_2\sigma^m$ and $C(\sigma) = C_1\sigma + C_2\sigma^p$. Using this form suggests that

Table 2 Apparent activation energy

Material	Q (kJ/mole)		
	31.5 MPa	56.5 MPa	73 MPa
332	173	246	284
332RR	137	131	122
333	152	125	356
M4032-2	193	190	272

Table 3 Parameters for nonrecoverable strain in viscous-viscoelastic creep/recovery model. Time t is in seconds

	$B_1(Pa^{-1}t^{-1/3})$	$B_2(Pa^{-m}t^{-1/3})$	m
M4032-2	5.11×10^{-9}	1.06×10^{-123}	14
332	5.49×10^{-8}	5.21×10^{-87}	10
332RR	8.29×10^{-11}	4.75×10^{-54}	6
333	1.72×10^{-10}	6.31×10^{-116}	13

Table 4 Parameters for recoverable strain in viscous-viscoelastic creep/recovery model. Time t is in seconds

	$C_1(Pa^{-1}t^{-1/3})$	$C_2(Pa^{-p}t^{-1/3})$	p
M4032-2	1.48×10^{-8}	0	–
332	4.77×10^{-8}	1.54×10^{-123}	14
332RR	6.70×10^{-11}	6.24×10^{-46}	5
333	9.40×10^{-11}	6.19×10^{-46}	5

at small stress, the material behaves linearly, while the second term becomes significant in the nonlinear regime. When determining the constants B_1, B_2, C_1, and C_2, it was also assumed that $B(\sigma = 0) = C(\sigma = 0) = 0$, since creep cannot occur under zero load. The values determined for the constants are given in Tables 3 and 4. The full model for creep and recovery is

$$\varepsilon(t) = \frac{\sigma}{E} + e^{\frac{-Q}{RT}}[(B_1\sigma + B_2\sigma^m) + (C_1\sigma + C_2\sigma^p)]t^n \quad 0 < t < t_1, \tag{9}$$

$$\varepsilon(t) = e^{\frac{-Q}{RT}}\left\{(B_1\sigma + B_2\sigma^m)t_1^n + (C_1\sigma + C_2\sigma^p)[t^n - (t - t_1)^n]\right\} \quad t > t_1 \tag{10}$$

The creep and recovery data from the 100000 second creep tests are shown with the model developed for each of the materials in Figs. 3–6. it is seen that at low to moderate stress, there is acceptable agreement between the viscous-viscoelastic model and experiment, but at high stress the error is large. This is a result of the apparent creep activation energy being much larger at 73 MPa for three of the four materials, as discussed previously. Agreement could be improved by removing the temperature compensated time and making multiple temperature specific models. It is also seen that at the largest loading at 260°C, the materials are entering the secondary creep regime, as the creep exponent n approaches 1. It is noted that due to the large amount of creep that occurs at the highest stress, especially at 260°C, that these types of conditions should be avoided in practice or the operating life of the engine will be drastically reduced.

Based on the model developed, the recoverable and nonrecoverable components of the creep strain can be plotted individually. This is shown over a period of six decades of time in
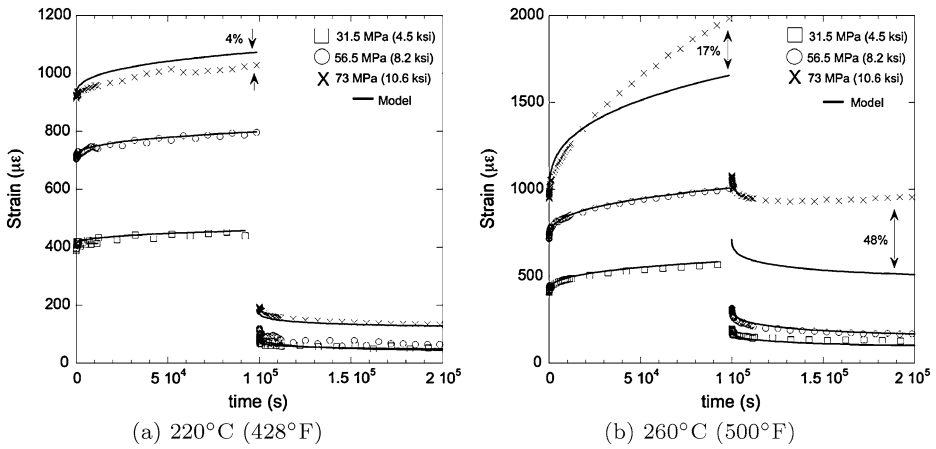
Fig. 3 Creep and recovery of M4032-2 alloy with viscous-viscoelastic model
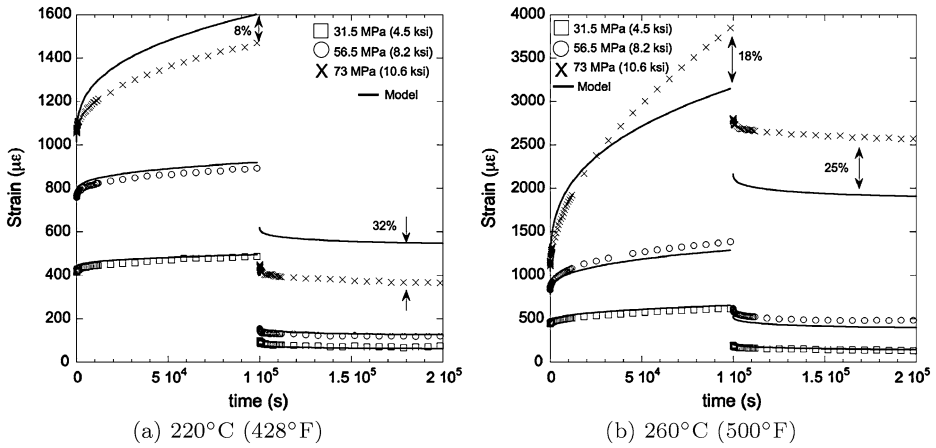

Fig. 4 Creep and recovery of 332 alloy with viscous-viscoelastic model

Fig. 7. The results for 73 MPa are omitted due to the inaccuracy of the model at this stress. From Fig. 7b it is seen that for 332 alloy, the nonrecoverable component of the creep strain is larger than the recoverable component throughout the stress and temperature range considered. Though not shown here, this was also the case for 332RR and 333 alloys (Dandrea 2008). For M4032-2 alloy, the converse is true (Fig. 7a).

It was mentioned earlier that the creep recovery of the material was investigated because it was considered to play a role in maintaining bolt load in a bolted joint. In practice the load is never fully removed, but partial unloading does occur. It has been shown in previous works that in an aluminum alloy joint held together with steel bolts, the stress in the aluminum increases above the initially applied stress when the joint is heated due to the differences in thermal expansion of the aluminum and steel. In some cases, the stress due to this thermal expansion is very large compared to the initially applied stress. Once at a constant temperature, the bolt load then begins to gradually decrease over time due to creep and relaxation. If the joint is then allowed to cool, the load in the joint is less than what is was
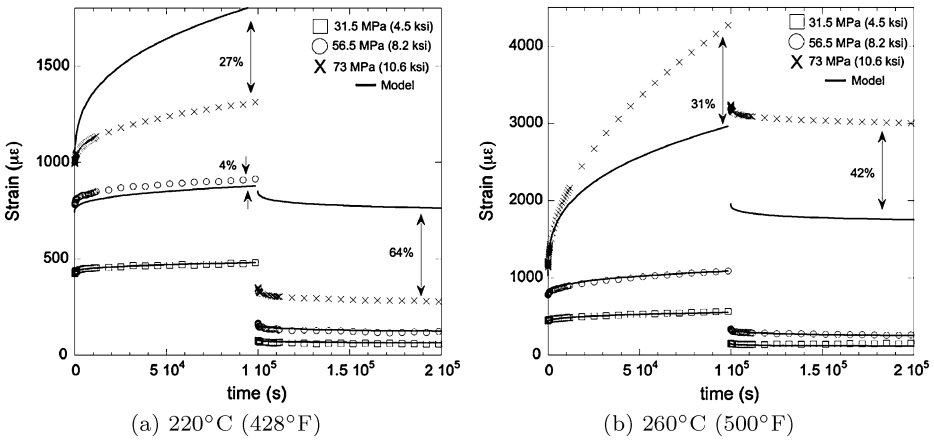
Fig. 5 Creep and recovery of 333 alloy with viscous-viscoelastic model
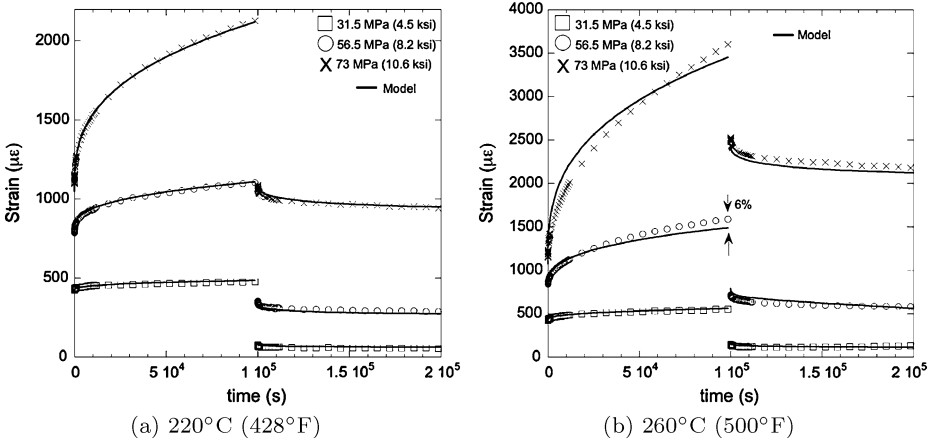

Fig. 6 Creep and recovery of 332RR alloy with viscous-viscoelastic model

initially (Jaglinski et al. 2007). It has been shown here that recovery occurs, and additional measurable creep over the time observed does not occur, when the load is reduced. There are then two possibilities that can occur when the material is partially unloaded: (1) the material undergoes recovery or (2) the material experiences a period of recovery followed by more creep. In the case of (1), the load loss in the joint will be primarily due to the permanent, nonrecoverable component, while in the case of (2) the load loss will be due to the total creep strain.

The model developed thus far does not account for the hardening that was seen to occur on subsequent loadings. Since in the application the material will see a number of thermal loading and unloading cycles, this hardening will occur in engine components and the model will become increasingly inaccurate over time. A full description of the hardening that occurs would require a large number of repeated creep tests on the same specimen, but an empirical method of addressing this phenomenon was created from the small num-
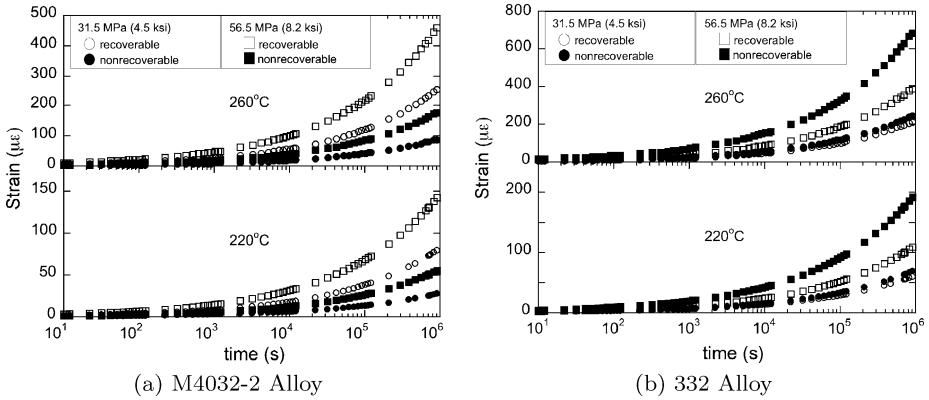
Fig. 7 Recoverable and nonrecoverable time-dependent strains for (**a**) M4032-2 and (**b**) 332 alloys based on viscous-viscoelastic model

ber of tests performed here. The method developed is unconventional, but provides engine designers with a simple method of predicting creep over a number of loading cycles.

It is shown in Fig. 2 that the strain rate is decreasing on subsequent loadings. For a material following a creep law of the form $\varepsilon(t) = \varepsilon_\circ + At^n$, the creep rate will be $\dot{\varepsilon} = nAt^{n-1}$. If we consider two subsequent loading and unloading cycles at a constant stress and temperature of a material that demonstrates the type of behavior seen here, the creep rate during the first loading will be $K_\circ t^{n-1}$ and during the second loading the creep rate will be $K_1 t^{n-1}$, where $K_1 < K_\circ$ and $K_i = nA_i$. Since $K_\circ$ and K_1 are constants, we can write K_1 as the product of two constants such that

$$K_1 = hK_\circ \tag{11}$$

It is proposed that the creep rate for any subsequent loading cycle can be represented by defining a dimensionless hardening parameter h which multiplies with the initial creep rate. The hardening parameter was taken to be a function of the total time t_t that the specimen has been under load. It is recalled that creep tests were performed, in succession, for times of 1000 s, 10000 s, and 100000 s. If $t_t = 0$ is set to coincide with the beginning of the 1000 second creep/recovery test. The strain rates during the 1000 second, 10000 second, and 100000 second creep tests at a given stress and temperature will then be $K_\circ t^{n-1}$, $K_1 t^{n-1}$, and $K_2 t^{n-1}$, respectively. It is assumed that n remains constant, so if the strain rate is decreasing $K_\circ > K_1 > K_2$. The constants $K_\circ, K_1,$ and K_2 can be determined by fitting the creep curve for each test to the form of $\varepsilon(t) = \varepsilon_\circ + At^n$ and taking the derivative. Then, by using the argument above

$$K_\circ = h(0)K_\circ, \tag{12}$$

$$K_1 = h(1000)K_\circ, \tag{13}$$

$$K_2 = h(11000)K_\circ \tag{14}$$

where it is assumed that $h(0) = 1$, and $h(1000)$ and $h(11000)$ can be determined by solving the above equations. The function $h(t_t)$ can then be determined from these three data points and was found could be represented by a function of the form

$$h(t_t) = \frac{1}{1 + Dt_t^q} \tag{15}$$

Table 5 Constants for hardening parameter $h(t_t)$

	D	q
332	0.04	0.31
332RR	0.14	0.23
333	0.16	0.23

where D and q are constants that can be determined from curve fitting. The creep of the material at any subsequent loading will then be given by

$$\varepsilon(t) = \varepsilon_\circ + h(t_t) A_\circ t^n \tag{16}$$

where $\varepsilon_\circ + A_\circ t^n$ describes the creep resulting from the initial loading. The values of the constants C and q determined for 332, 332RR and 333 alloys are given in Table 5. Minimal hardening was observed in M4032-2 alloy.

3.2 Materials comparison

The engine manufacturer would like to use materials that are as creep resistant as possible, balanced against other required material properties, manufacturing processability, and cost. For this reason the materials studied here are compared in terms of creep performance. Differences in creep rates between different aluminum alloys is a result of alloy composition and variations in the casting processes used by different manufacturers. Creep of the four materials over a period of 100000 seconds (~28 hours) are shown together in Fig. 8. At the 31.5 MPa stress level all of the materials showed nearly identical creep rates at both 220° and 260°, so these tests are omitted from the plots. For the three permanent mold cast materials from the same manufacturer, at 56.5 MPa and 220°C, the 332RR alloy begins to show a significant amount of creep, while 332 and 333 alloys remain similar. At a stress of 56.5 MPa and temperature of 260°C, 333 alloy is the best performer while 332 and 332RR alloys show similar amounts of creep. At the highest loading at 260°C, the creep rate of all three materials increases drastically. At these conditions, failure would likely occur quite rapidly. It is concluded that of these three materials, 333 alloy has the best resistance to creep and 332RR has the worst. Over the entire range of stress/temperature, the die-cast M4032-2 alloy shows the least amount of creep. The relative differences in performance between the four alloys is likely due to a combination of differences in chemistry, casting, and heat treatment processing, which give rise to different microstructures. The influence of microstructural attributes on the differences in creep and recovery performance should be the subject of further study.

4 Conclusions

Constant load uniaxial creep tests were performed on four aluminum alloys for small engines. The creep tests were performed for periods of 100 seconds, 1000 seconds, 10000 seconds, and 100000 seconds at initial stress levels of 31.5 MPa (4.5 ksi), 56.5 MPa (8.2 ksi), and 73 MPa (10.6 ksi). Tests at each stress level were completed at both 220°C (428°F) and 260°C (500°F). Following each creep test, the load was removed and the creep recovery of the material was observed. The creep and recovery was modeled using a viscous-viscoelastic model and incorporated temperature compensated time. The model showed good agreement
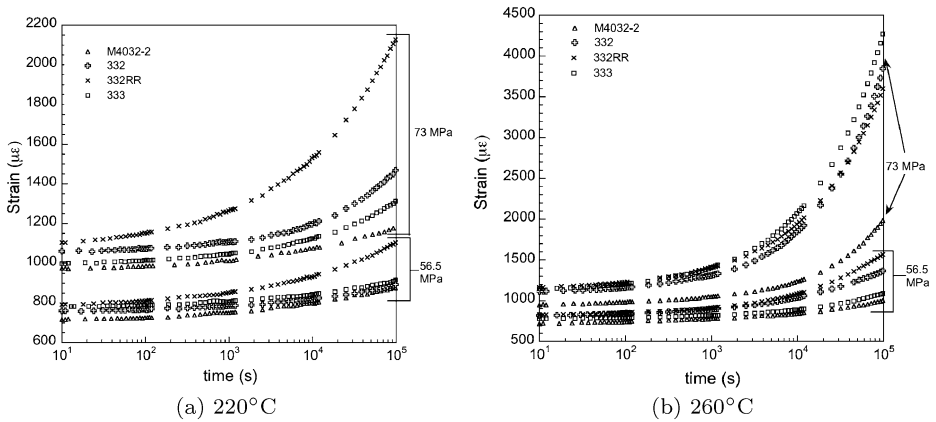
Fig. 8 Creep comparison of 332, 332RR, 333, and M4032-2 alloys

with experiment at stresses 31.5 MPa and 56.5 MPa, but deviated at the highest loading due to the apparent creep activation energy increasing by a large amount at this stress.

Repeated loading of the same specimen revealed that hardening, indicated by a decreasing creep rate on subsequent loadings, occurs in 332, 332RR, and 333 alloys. This was also seen in M4032-2 alloy, but to a much lesser extent. This hardening improves the creep performance of the material and suggests that preconditioning the engine would improve its long term reliability. An empirical method was developed for incorporating this hardening into the creep model developed

The creep performance, illustrated by the total amount of strain over the length of the creep tests, of the materials tested was compared. The material with the best resistance to creep over the entire range of stress and temperature was the M4032-2 alloy. All of the materials tested were highly nonlinear at a stress of 73 MPa at 260°C. For the three permanent mold cast materials supplied by the same manufacturer for creep testing, it was found that over the entire range of stress and temperature, the material with the best creep performance was 333 alloy. The material with the least resistance to creep was 332RR alloy.

The approach used here may be applicable to other materials.

References

Andrade, E.N.: On the viscous flow in metals and allied phenomena. Proc. R. Soc. Lond., Ser. A: Contain. Pap. Math. Phys. Character **84**(567), 1–12 (1910)

Cho, U.W., Findley, W.N.: Creep and creep recovery of 304 stainless steel under combined stress with a representation by a viscous-viscoelastic model. Trans. ASME: J. Appl. Mech. **47**(4), 755–761 (1980)

Cho, U.W., Findley, W.N.: Creep and plastic strains of 304 stainless steel at 593°C under step stress changes, considering aging. Trans. ASME: J. Appl. Mech. **49**(2), 297–304 (1982)

Cho, U.W., Findley, W.N.: Creep and creep recovery of 2618-T61 aluminum under variable temperature. Trans. ASME: J. Appl. Mech. **51**(4), 816–820 (1984)

Dandrea, J.: Nonlinear creep and creep recovery of die-cast aluminum alloys. M.S. Thesis, Univ. of Wisconsin-Madison (2008)

Ding, J.L., Findley, W.N.: Nonproportional loading steps in multiaxial creep of 2618 aluminum. Trans. ASME: J. Appl. Mech. **52**(3), 621–628 (1985)

Findley, W.N., Lai, J.S.Y.: A modified superposition principle applied to creep of nonlinear viscoelastic material under abrupt changes in state of combined stress. Trans. Soc. Rheol. **11**(3), 361–380 (1967)

Findley, W.N., Lai, J.S.: Creep and recovery of 2618 aluminum alloy under combined stress with a representation by a viscous-viscoelastic model. Trans. ASME: J. Appl. Mech. **45**(3), 507–514 (1978)

Jaglinski, T., Lakes, R.S.: Creep behavior of Al-Si die-cast alloys. J. Eng. Mater. Technol. **126**(4), 378–382 (2004)

Jaglinski, T., Nimityongskul, A., Schmitz, R., Lakes, R.S.: Study of bolt load loss in bolted aluminum joints. J. Eng. Mater. Technol. **129**(1), 48–54 (2007)

Nimityongskul, A.: Creep and relaxation in die-cast aluminum alloys at elevated temperature. M.S. Thesis, Univ. of Wisconsin-Madison (2005)

Sherby, O.D., Orr, R.L., Dorn, J.E.: Creep correlations of metals at elevated temperatures. J. Met. **6**(1), 71–80 (1954)